



Histidine-rich glycoprotein possesses antioxidant activity through self-oxidation and inhibition of hydroxyl radical production via chelating divalent metal ions in Fenton's reaction

Hidenori Wake , Yohei Takahashi , Yukinori Yoshii , Shangze Gao , Shuji Mori , Dengli Wang , Kiyoshi Teshigawara & Masahiro Nishibori

To cite this article: Hidenori Wake , Yohei Takahashi , Yukinori Yoshii , Shangze Gao , Shuji Mori , Dengli Wang , Kiyoshi Teshigawara & Masahiro Nishibori (2020): Histidine-rich glycoprotein possesses antioxidant activity through self-oxidation and inhibition of hydroxyl radical production via chelating divalent metal ions in Fenton's reaction, Free Radical Research, DOI: [10.1080/10715762.2020.1825703](https://doi.org/10.1080/10715762.2020.1825703)

To link to this article: <https://doi.org/10.1080/10715762.2020.1825703>



© 2020 The Author(s). Published by Informa UK Limited, trading as Taylor & Francis Group.



[View supplementary material](#)



Published online: 06 Oct 2020.



[Submit your article to this journal](#)



Article views: 184



[View related articles](#)



[View Crossmark data](#)

Histidine-rich glycoprotein possesses antioxidant activity through self-oxidation and inhibition of hydroxyl radical production via chelating divalent metal ions in Fenton's reaction

Hidenori Wake^a, Yohei Takahashi^a, Yukinori Yoshii^a, Shangze Gao^a, Shuji Mori^b, Dengli Wang^a, Kiyoshi Teshigawara^a and Masahiro Nishibori^a

^aDepartment of Pharmacology, Okayama University Graduate School of Medicine, Dentistry, and Pharmaceutical Sciences, Okayama, Japan; ^bDepartment of Pharmacology, Shujitsu University School of Pharmacy, Okayama, Japan

ABSTRACT

Sepsis is caused by infections associated with life-threatening multiple organ failure (MOF). Septic MOF appears to be closely related to circulatory failure due to immunothrombosis. This process involves the production of reactive oxygen species (ROS) in inflammatory sites. Therefore, the detoxification of the systemic excess ROS is important for the improvement of the process in septic pathogenesis. Histidine-rich glycoprotein (HRG), a plasma glycoprotein, ameliorates a septic condition through the suppression of both excess ROS production from neutrophils and immunothrombosis. Hydroxyl radical is known as the most important species among ROS in pathogenesis; however, the direct influence of HRG on hydroxyl radical formation and ROS activity is poorly understood. In this study, we showed that HRG, in a concentration-dependent manner, efficiently inhibited the production of hydroxyl radical induced by the Fenton's reaction through chelation of the divalent iron. HRG also exhibited antioxidant activity against peroxy radical by oxidation of HRG itself as a substrate; however, it did not show superoxide dismutase and catalase-like activities. Additionally, HRG enhanced glutathione peroxidase, a well-known antioxidant enzyme, activity. These results suggest that HRG may play a unique role in suppression of the production of hydroxyl radicals and subsequent tissue damage at inflammatory sites. Marked reduction in plasma HRG in sepsis might lose such an important protective mechanism. Thus, the present study provides evidence that inhibition of ROS and ROS-production systems by HRG may contribute to antiseptic effects *in vivo* and that HRG could be potential therapy for ROS-related diseases.

ARTICLE HISTORY

Received 15 June 2020
Revised 8 September 2020
Accepted 14 September 2020

KEYWORDS



Histidine-rich glycoprotein; reactive oxygen species; Fenton's reaction; divalent metal ions; sepsis


Introduction

Sepsis is the leading cause of death in the intensive care unit (ICU), and 20~30 million people develop sepsis annually worldwide [1,2]. Although there have been several clinical trials to evaluate the novel therapies for sepsis, including anti-cytokines and anti-innate immune reactions for decades, all of them have failed to demonstrate the beneficial effects in patients [3–6]. The lethality of sepsis remains around 25% even in ICU, and the sepsis campaign for overcoming the situation continues worldwide [1,7,8], necessitating a novel approach of drug designing.

The pathological progress of sepsis includes respiratory failure, circulatory shock, immune paralysis, and

disseminated intravascular coagulation induced by the systemic response to the infection of bacteria, viruses, or fungi that may lead to the mortality and morbidity [9,10]. It is considered that the disorder of the interaction between blood cells and vascular endothelial cells occur in septic condition, associated with the pro-coagulant state and that immunothrombosis may be important for the pathogenesis of multiple organ failure [11–13]. Immunothrombosis is the formation of blood clots triggered by adhesion of activated neutrophils to vascular endothelial cells stimulated by bacterial infections [14]. Adherent neutrophils on endothelial cells produce reactive oxygen species (ROS) and induce the generation of ROS by the surrounding cells, such as

CONTACT Masahiro Nishibori  mbori@md.okayama-u.ac.jp  Department of Pharmacology, Okayama University Graduate School of Medicine, Dentistry, and Pharmaceutical Sciences, Okayama 700-8558, Japan

 Supplemental data for this article is available online at <https://doi.org/10.1080/10715762.2020.1825703>.

© 2020 The Author(s). Published by Informa UK Limited, trading as Taylor & Francis Group.

This is an Open Access article distributed under the terms of the Creative Commons Attribution-NonCommercial-NoDerivatives License (<http://creativecommons.org/licenses/by-nc-nd/4.0/>), which permits non-commercial re-use, distribution, and reproduction in any medium, provided the original work is properly cited, and is not altered, transformed, or built upon in any way.

endothelial cells. The neutrophils also release neutrophil extracellular traps (NETs) in infectious inflammation resulting in the inhibition of bacterial diffusion into the bloodstream [15]. Platelets accumulate and adhere to the neutrophils and NETs, followed by aggregatory and secretory responses. Furthermore, the release of Zn^{2+} from platelets may facilitate the aggregation of erythrocytes forming fibrin clots. Although the immunothrombosis has been thought to contribute to the containment of bacteria and bacterial killing, the thrombi lead to ischemic/hypoxic condition in multiple organs and tissue injury caused by ROS once the thrombus is formed randomly in the whole body due to impairment in the regulation of immunothrombosis in systemic septic inflammation [16–18]. Besides, it is thought that ROS plays a critical role in the systemic inflammation, the NETs release in thrombi formation and the tissue peroxidation, and so forth. [11,12,16–18].

Histidine-rich glycoprotein (HRG) is a 75 kDa plasma glycoprotein produced in the liver and exists at around 1 μ M in human plasma [19,20]. HRG consists of four domain structures (cystatin-like domain 1, cystatin-like domain 2, histidine-rich domain, C-terminal domain) [19,20]. Histidine-rich domain has a unique 12 GHHPH tandem repeat subsequence [21], and HRG is known to bind to several ligands that determine its activities. Through binding to heparin, fibrin, and fibrinogen or plasmin and plasminogen, HRG exerts an anticoagulant and anti-fibrinolysis activities, respectively [22–25]. The binding of HRG to dead cells and toxic substances such as heme and lipopolysaccharide supports scavenging and toxin neutralization [26–29]. Moreover, its association with *in vivo* kinetics of divalent metal ions is due to the binding to zinc, nickel, cobalt, copper, mercury, and cadmium [30,31].

We previously reported that plasma HRG levels were significantly decreased in cecal ligation and puncture (CLP) septic mouse model. The survival rate of CLP mice was reduced in HRG knock-down mice by RNAi method, and HRG supplementary therapy in septic conditions led to ameliorate its survival rate [32]. In a clinical setting, plasma HRG levels in septic patients were also decreased significantly compared with healthy volunteers, as observed in the CLP mouse model [32,33]. The results suggested that HRG is a useful prognosis prediction marker of sepsis and plays a critical role in the prevention of the pathogenesis of sepsis. Furthermore, HRG maintains the quiescence of neutrophils through the regulation of their shapes and spontaneous ROS production and the easy passage through microcapillaries [32]. These results as a whole revealed that HRG ameliorates septic pathogenesis due to cellular

regulation of neutrophils and vascular endothelial cells, resulting in suppression of the immunothrombus formation and protection of vascular endothelial cell damage by ROS produced by neutrophils [32]. However, the direct effects of HRG on cell-free ROS-production system and ROS scavenging capacity were poorly understood. In this study, we investigated the effects of HRG on Fenton's reaction and ROS-neutralizing activity *in vitro* to better understand the profile of the antiseptic effects of HRG.

Materials and methods

Reagents

Iron (II) sulfate, Iron (III) sulfate, Cobalt (II) sulfate, Zinc (II) sulfate, Copper (II) sulfate, Nickel (II) sulfate, GHHPHGHHPH peptide, GAAPAGAAPA peptide, and Human serum albumin (HSA) were obtained from Sigma-Aldrich (St. Louis, MO).

Purification of HRG from human plasma

Human HRG was purified from human fresh frozen plasma (Japanese Red Cross Society, Okayama, Japan) as described previously [34]. In brief, human plasma containing protease inhibitors was incubated with nickel-nitrilotriacetic acid agarose (Qiagen, Hilden, Germany) for 2 h at 4 °C with gentle shaking. The gel was packed into a column and washed with 10 mM Tris-buffered saline (TBS; pH 8.0) containing 50 mM imidazole and 10 mM Tris-buffer (pH 8.0) containing 2 M NaCl. HRG fraction was eluted by 0.5 M imidazole in 10 mM TBS (pH 8.0). The eluate was further purified by a Mono Q column (GE Healthcare, Little Chalfont, UK) with a NaCl gradient. Purified HRG was dialyzed against phosphate-buffered saline (PBS) and identified by Western blotting with a rabbit polyclonal antibody against human HRG (produced in our lab). The contents of metals in purified HRG (1 μ M) were measured by Atomic Absorption Spectrophotometer Z-9000 (Hitachi, Tokyo, Japan). We found the very low levels of metals in the preparation; Fe: 0.97 ppb, Co: 3.6 ppb, Zn: 11.7 ppb, Cu: N.D., and Ni: 25 ppb.

Measurement of superoxide antioxidant activity

The superoxide scavenging ability of HRG was determined using a DetectX superoxide dismutase (SOD) colorimetric activity kit (Arbor Assays, Ann Arbor, MI) according to the manufacturer's instruction. The SOD standard or HRG was incubated with the substrate and the xanthine oxidase solution for 20 min at RT (21–23 °C). The absorbance was read at 450 nm.

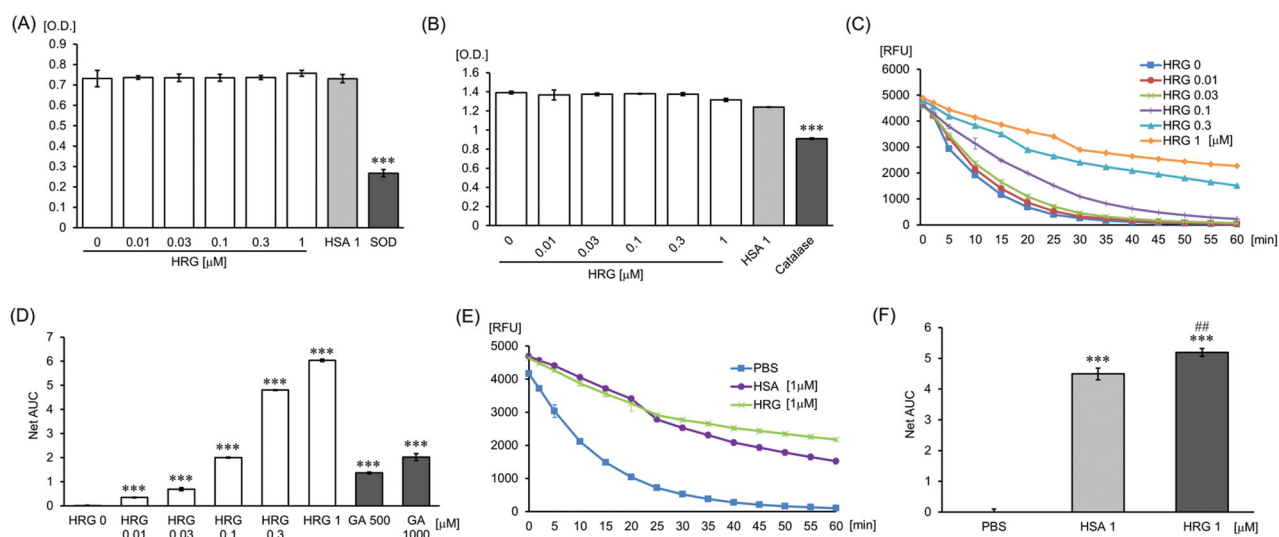


Figure 1. Effects of HRG on superoxide, hydrogen peroxide, and hydroxyl radical. (A) HRG's effect on superoxide. HRG (0–1 μM), HSA (1 μM) or SOD standard (0.1 unit/ml) was incubated with the substrate and the xanthine oxidase solution for 20 min at RT. The absorbance was read at 450 nm. (B) HRG's effect on hydrogen peroxide. HRG (0–1 μM), HSA (1 μM) or catalase standard (0.7 unit/ml) was incubated with Hydrogen Peroxide Working Solution (H_2O_2) for 1 min at RT followed by incubation with chromogenic working solution for 60 min at RT. The absorbance was detected at 520 nm. The results shown are the means \pm SEM of three experiments. *** $p < 0.001$ vs. PBS (HRG 0 μM). (C–F) HRG's effect on hydrogen peroxide. The quenching curve of the fluorescent probe in HRG (0–1 μM) (C) or in the group treated with PBS, HSA (1 μM), or HRG (1 μM) (E). The antioxidant capacity was calculated on the basis of the area under the fluorescent decay curve shown in (D) and (F). Gallic acid as positive control. The results shown are the means \pm SEM of three experiments. *** $p < 0.001$ vs. PBS (HRG 0 μM). ## $p < 0.01$ vs. HSA.

Measurement of hydrogen peroxide antioxidant activity

The hydrogen peroxide scavenging ability of HRG was determined using an OxiSelect catalase activity assay kit (Cell Biolabs, San Diego, CA) according to the manufacturer's instruction. The catalase standard or HRG was incubated with Hydrogen Peroxide Working Solution (H_2O_2) for 1 min at RT, followed by incubation with chromogenic working solution for 60 min at RT. The absorbance was detected at 520 nm.

Hydroxyl radical antioxidant capacity activity and oxygen radical antioxidant capacity activity assay

The hydroxyl radical antioxidant capacity (HORAC) activity of HRG was determined using an OxiSelect HORAC activity assay kit (Cell Biolabs), and the oxygen radical antioxidant capacity (ORAC) activity of HRG was determined using an OxiSelect ORAC activity assay kit (Cell Biolabs) according to the manufacturer's instruction. The HORAC assay is based on the oxidation-mediated quenching of a fluorescent probe by hydroxyl radical produced by hydroxyl radical initiator (H_2O_2) and Fenton reagent. The ORAC assay is based on the oxidation-mediated quenching of a fluorescent probe by peroxy radicals produced by a free radical initiator [AAPH: 2,2'-Azobis(2-amidinopropane) dihydrochloride].

Antioxidants delay the quenching of the fluorescent probe. The antioxidant capacity was calculated on the basis of the area under the fluorescent decay curve (Net AUC = AUC (Antioxidant) – AUC (blank)). Gallic acid (for HORAC) and Trolox (for ORAC) were used as positive controls.

Isothermal titration calorimetry assay

Isothermal titration calorimetry (ITC) experiments were performed at 25 $^{\circ}\text{C}$ using Microcal iTC200 (GE Healthcare). On the one hand, an appropriate amount of HRG (0.033 mM in PBS), HSA (0.033 mM in PBS), or PBS (buffer control) was loaded in a sample cell. Eighteen successive 2 μl aliquots of FeSO_4 (10 mM), $\text{Fe}_2(\text{SO}_4)_3$ (5 mM), CoSO_4 (2.5 mM), ZnSO_4 (5 mM), CuSO_4 (2.5 mM), or NiSO_4 (2.5 mM) was titrated into the sample cell.

In contrast, an appropriate amount of 2GHHPH peptide (0.2 mM in PBS), 2GAAPA peptide (0.2 mM in PBS) or PBS (buffer control) was loaded in a sample cell. Eighteen successive 2 μl aliquots of FeSO_4 (7.5 mM), $\text{Fe}_2(\text{SO}_4)_3$ (5 mM), CoSO_4 (0.625 mM), ZnSO_4 (2.5 mM), CuSO_4 (1.25 mM) or NiSO_4 (1.25 mM) was titrated into the sample cell.

The duration of each injection was 4 s, and the interval between injections was 120 s. The final data were

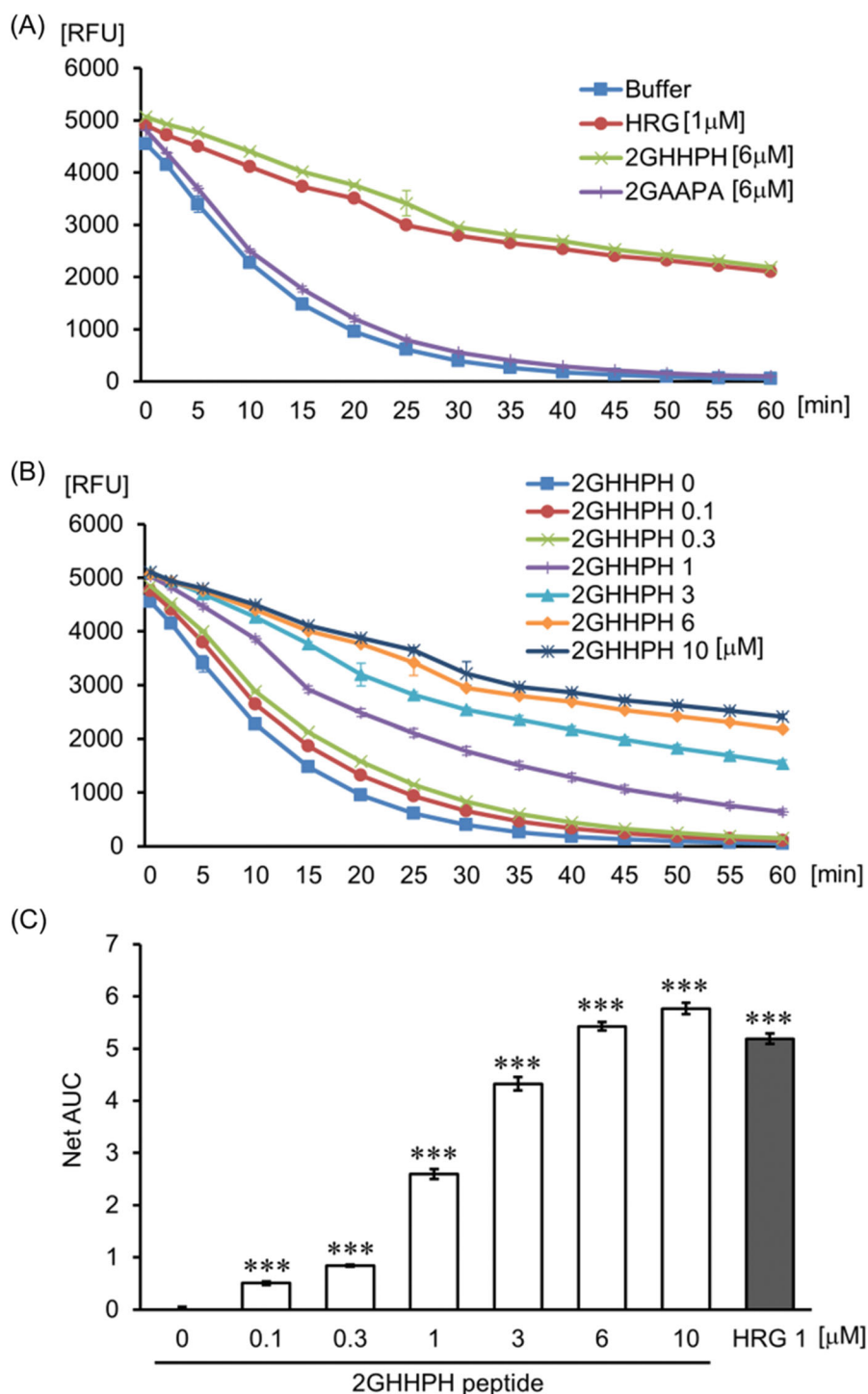


Figure 2. The effect of GHHPH peptide on hydroxyl radicals. (A) The quenching curve of the fluorescent probe in the group treated with PBS, HRG (1 μM), 2GHHPH (6 μM), and 2GAAPA (6 μM). (B) The curve obtained for the different concentrations of 2GHHPH (0–10 μM). (C) The antioxidant capacity was calculated on the basis of the area under the fluorescent decay curve. The results shown are the means ± SEM of three experiments. *** $p < 0.001$ vs. PBS (2GHHPH peptide 0 μM).

corrected by subtracting the data of metal ion from PBS and analyzed by using Origin software 7.0 (GE Healthcare).

Detection of oxidized HRG

The protein carbonyls were detected using an OxiSelect protein carbonyl fluorometric assay kit (Cell Biolabs)

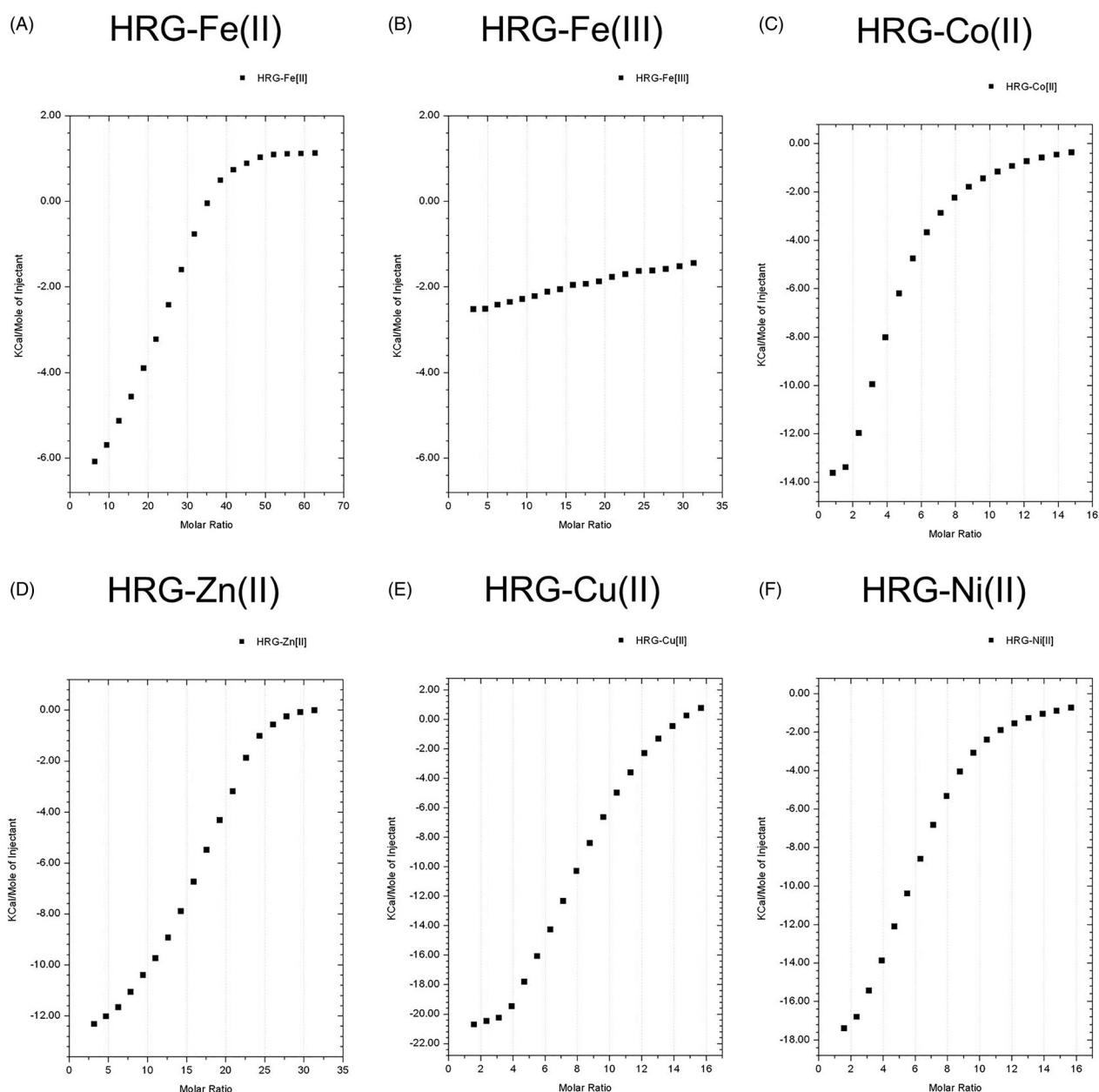


Figure 3. The binding ability of HRG to divalent metal. ITC experiments were performed at 25 °C using Microcal iTC200 to determine the binding ability of HRG to - (A) FeSO_4 (10 mM), (B) $\text{Fe}_2(\text{SO}_4)_3$ (5 mM), (C) CoSO_4 (2.5 mM), (D) ZnSO_4 (5 mM), (E) CuSO_4 (2.5 mM), and (F) NiSO_4 (2.5 mM). The final data were corrected by subtracting the data of metal ion into PBS.

according to the manufacturer's instruction. Proteins were oxidized by peroxy radicals produced by AAPH, and the oxidized protein was mixed with protein carbonyl fluorophore. The fluorescence was detected at Ex 485/Em 530. Protein concentration was determined using the Bradford assay, and the results were represented as nmol of protein carbonyl per mg of protein.

Modification of protein thiols was detected using a Protein Redox State Monitoring kit (Dojindo, Kumamoto, Japan) according to the manufacturer's instruction. The protein thiols were labeled with Protein-SHifter (15 kDa), which has a maleimide group.

The protein methionine sulfoxide (MetO) as an oxidized methionine was detected with a rabbit anti-MetO polyclonal antibody (Methionine Sulfoxide Immunoblotting Kit: Cayman Chemical, Ann Arbor, MI).

The di-tyrosine (DT) as an oxidized tyrosine was detected with mouse anti-DT monoclonal antibody (clone 1C3: Nikken seil, Shizuoka, Japan).

Glutathione peroxidase assay

The glutathione peroxidase (GPx)-like activity of HRG was measured using Amplitude Fluorimetric Glutathione

Table 1. Analysis data of HRG binding to metal ion.

| Model: one sites | <i>N</i> | <i>K_A</i> |
|------------------|------------------|---------------------------------|
| HRG-Fe[II] | 22.1 ± 1.6 sites | 6.40E4 ± 5.70E4 M ⁻¹ |
| HRG-Fe[III] | — | — |
| HRG-Co[II] | 4.2 ± 0.07 sites | 3.81E4 ± 2.79E3 M ⁻¹ |
| HRG-Zn[II] | 16.3 ± 0.3 sites | 4.73E4 ± 8.12E3 M ⁻¹ |
| HRG-Cu[II] | 7.7 ± 0.2 sites | 7.53E4 ± 1.35E4 M ⁻¹ |
| HRG-Ni[II] | 6.0 ± 0.04 sites | 4.26E4 ± 1.40E3 M ⁻¹ |

N: binding stoichiometry; *K_A*: association constant.

Peroxidase Assay Kit (AAT Bioquest, Sunnyvale, CA) according to the manufacturer's instruction. This assay is based on the oxidation of glutathione (GSH) to oxidized glutathione (GSSG) catalyzed by GPx with hydrogen peroxide. The GSSG is recycled to GSH by glutathione reductase (GR) and NADPH, which leads to NADP⁺ generation. The generated NADP⁺ is detected by the NADP sensor. Briefly, PBS, HSA (1 μM) or HRG (1 μM), or GPx standard (0–40 mU/ml) with PBS, HSA (1 μM), or HRG (1 μM) was mixed with GPx working solution and incubated at room temperature for 30 min. Subsequently, the Quest Fluor NADP probe and NADP assay solution were added and incubated at room temperature for 20 min, followed by additional incubation for 20 min with the enhancer solution. The NADP probe reacted with NADP⁺-derived fluorescence was measured at Ex 420 nm and Em 480 nm. GPx enhancing capacity was represented with Net RFU (Net RFU = RFU (Sample + GPx) – RFU (Sample)).

Surface plasmon resonance (SPR) assay

SPR experiments were performed at 25 °C using Biacore T200 (GE Healthcare). HRG was immobilized on CM5 sensor chip (GE Healthcare). Increasing concentrations of the recombinant GPx proteins (GPx1, GPx3, and GPx4; abcam, Cambridge, UK) dissolved in HBS-EP + buffer (GE Healthcare) were injected at a flow rate of 30 μl/min for 120 s. After that, dissociation was evaluated by passing the buffer alone over the chip for 120 s. The binding kinetics were analyzed using Biacore T200 Evaluation software (GE Healthcare).

Neutrophil rounding assay

Neutrophils were isolated with density-gradient method using Polymorphprep (Axis-Shield, Oslo, Norway). Neutrophils were pre-stained with Hoechst33342 (Nuclei; Thermo Fisher Scientific) and Calcein-AM (Cytosol) (Thermo Fisher Scientific), aliquoted to 96 wells plate (Corning, Riverfront Plaza, NY) and stimulated by HBSS, HRG (1 μM), and oxidized HRG (1 μM), which was oxidized by AAPH at RT for 1 h and dialyzed against PBS, at 37 °C for 1 h. Neutrophil morphology

was observed by an In Cell Analyzer 2000 (GE Healthcare) and analyzed by In Cell Analyzer Workstation software (GE Healthcare). Form factor (max diameter/min diameter) was determined.

Statistical analysis

The statistical analysis across multiple treatment groups was determined with ANOVA, followed by Tukey test. All data are presented as the means ± standard error (SEM). *p* Values < 0.05 were considered statistically significant.

Results

Effects of HRG on superoxide and hydrogen peroxide

To investigate the action of HRG on superoxide, we used a superoxide production system composed of xanthine, oxygen, and xanthine oxidase. SOD catalyzed the dismutation of superoxide to oxygen and hydrogen peroxide as the positive control. The results revealed that the HRG had no effect on the superoxide-production system and did not show SOD-like activity (Figure 1(A)). HSA, known as possessing antioxidant activity through self-oxidation, also had no effect on those (Figure 1(A)). To examine the effect of HRG on hydrogen peroxide, we investigated whether HRG has the catalyzing activity on hydrogen peroxide by incubation of HRG and hydrogen peroxide. Catalase catalyzed hydrogen peroxide into water and oxygen as the positive control; however, we could not detect any catalyzing activity of HRG on hydrogen peroxide (Figure 1(B)). HSA also did not show catalyzing activity on hydrogen peroxide (Figure 1(B)).

HORAC activity of HRG

The effects of HRG on hydroxyl radical production were examined by the HORAC assay. Gallic acid as positive control exhibited antioxidant activity on hydroxyl radical production (Figure 1(D) and Supporting Information Fig. 1). HRG inhibited the fluorescent quenching by hydroxyl radical in a concentration-dependent manner (Figure 1(C,D)). Figure 2(A–C) shows that the GHHPH repeat sequence of HRG inside the histidine-rich domain produced a similar concentration-dependent inhibitory effect of fluorescent quenching by hydroxyl radical, whereas 2GAAPA peptide replacing histidine residues of 2GHHPH peptide with alanine did not show antioxidant activity (Figure 2(A)). In comparison to HSA, HRG have significantly higher antioxidant

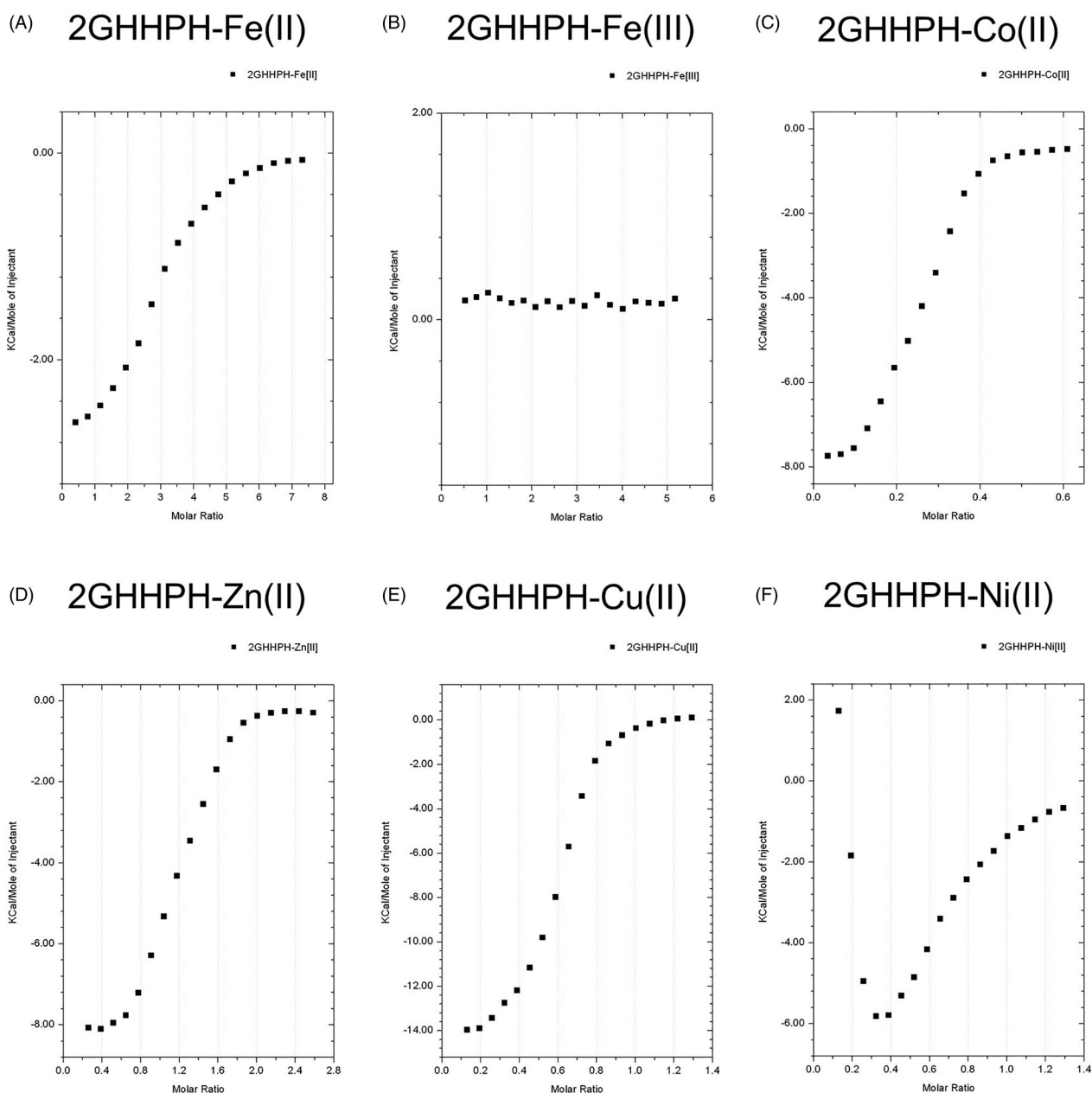


Figure 4. The binding ability of GHHPH peptide to divalent metal. ITC experiments were performed at 25 °C using Microcal iTC200 to determine the binding ability of 2GHHPH peptide to - (A) FeSO_4 (7.5 mM), (B) $\text{Fe}_2(\text{SO}_4)_3$ (5 mM), (C) CoSO_4 (0.625 mM), (D) ZnSO_4 (2.5 mM), (E) CuSO_4 (1.25 mM), and (F) NiSO_4 (1.25 mM). The final data were corrected by subtracting the data of metal ion into PBS.

Table 2. Analysis data of GHHPH peptide binding to metal ion.

| Model: one sites | N | K_A |
|------------------|-----------------------|--|
| 2GHHPH-Fe[II] | 2.9 ± 0.02 sites | $2.00\text{E}4 \pm 1.13\text{E}3 \text{ M}^{-1}$ |
| 2GHHPH-Fe[III] | — | — |
| 2GHHPH-Co[II] | 0.3 ± 0.003 sites | $2.73\text{E}5 \pm 2.63\text{E}4 \text{ M}^{-1}$ |
| 2GHHPH-Zn[II] | 1.2 ± 0.01 sites | $1.08\text{E}5 \pm 1.14\text{E}4 \text{ M}^{-1}$ |
| 2GHHPH-Cu[II] | 0.6 ± 0.006 sites | $3.83\text{E}5 \pm 4.59\text{E}4 \text{ M}^{-1}$ |
| Model: two sites | N | K_A |
| 2GHHPH-Ni[II] 1 | 0.2 ± 0.4 sites | $3.70\text{E}4 \pm 3.55\text{E}4 \text{ M}^{-1}$ |
| 2GHHPH-Ni[II] 2 | 0.2 ± 0.1 sites | $1.12\text{E}5 \pm 3.22\text{E}5 \text{ M}^{-1}$ |

N : binding stoichiometry; K_A : association constant.

activity on hydroxyl radical (Figure 1(E,F)). In addition, the effect of HRG-Fe^{2+} complex on hydroxyl radical production was examined by allowing the complex formation by pre-incubation of HRG with Fe^{2+} for 30 min in the HORAC assay. We could not observe the difference in the inhibition level of fluorescence quenching by hydroxyl radical between pre-incubation group and non-pre-incubation group (Supporting Information Fig. 2). These data indicated that HRG-Fe^{2+} complex did not induce Fenton's reaction.

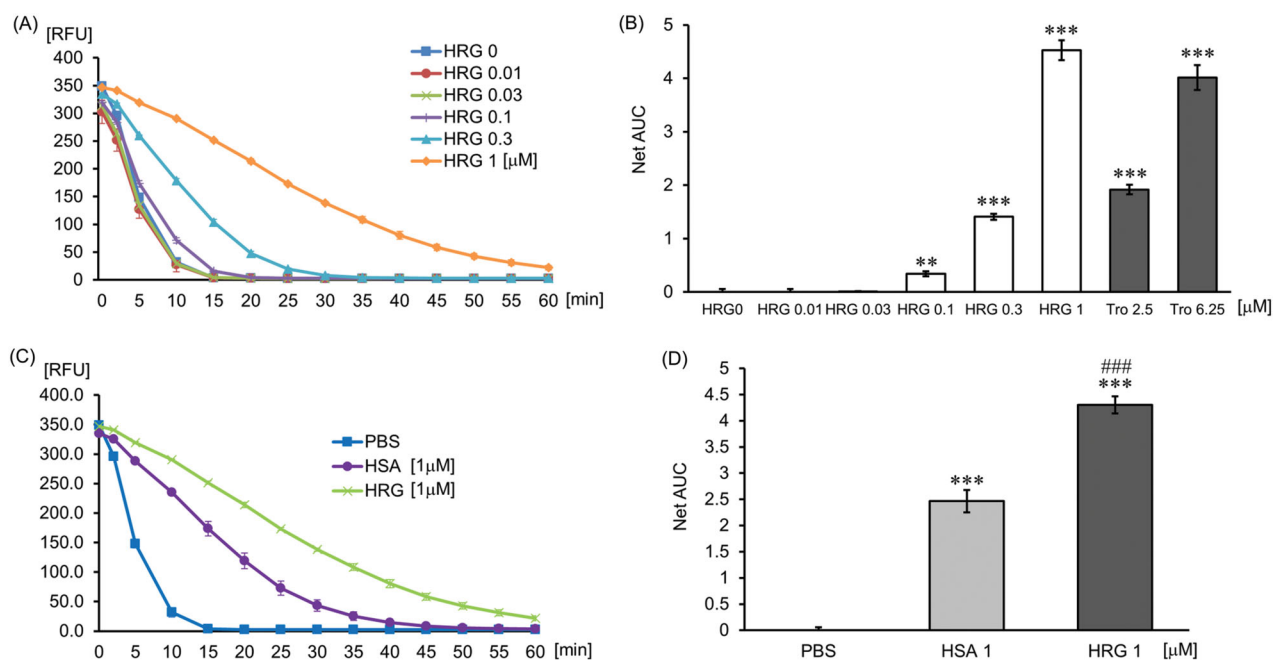


Figure 5. The effect of HRG on peroxy radical. The quenching curve of the fluorescent probe in a concentration-dependent manner (HRG 0–1 μM) (A) or in the group treated with PBS, HSA (1 μM), or HRG (1 μM) (C). The antioxidant capacity was calculated on the basis of the area under the fluorescent decay curve (B and D). Trolox is positive control as antioxidant. The results shown are the means ± SEM of three experiments. *** $p < 0.001$ vs. PBS (HRG 0 μM). ### $p < 0.001$ vs. HSA.

The binding ability of HRG and HRG-derived peptide to metal ions

We performed ITC assay to determine the binding ability of HRG to metal ions (ex. Fe^{2+} and Co^{2+} , the essential factors in Fenton's reaction). The results revealed that HRG could bind to divalent metal ions (Fe^{2+} , Cu^{2+} , Co^{2+} , Zn^{2+} , Ni^{2+}) with an intermediate affinity ($K_A = 3.81\text{E}4 \sim 7.53\text{E}4$). However, HRG cannot bind to Fe^{3+} . One molecule of HRG can bind to 4–22 molecules of divalent metal ions with a higher binding affinity for divalent iron ion more as compared with the other divalent metal ions (Figure 3 and Table 1). 2GHHPH repeat sequence is the core of HRG binding to divalent metal ions, and histidine residue of GHHPH peptide is bound to Fe^{2+} , whereas 2GAAPA did not, suggesting an essential role of histidine residues for those binding (Figure 4, Table 2, and Supporting Information Fig. 3). HSA, at the same concentration (1 μM) of HRG, did not bind to metal ions in the tested concentrations (Supporting Information Fig. 4).

ORAC activity of HRG

To examine the effect of HRG on the action of peroxy radical, we performed ORAC assay. Trolox, as a positive control, showed significant antioxidant activity on peroxy radical (Figure 5(B) and Supporting Information

Fig. 5), whereas HRG inhibited the fluorescent quenching by peroxy radicals in a concentration-dependent manner (Figure 5(A,B)). The 2GHHPH peptide had weak antioxidant activity on this assay system (Figure 6(A–C)). Compared with HRG, HSA showed weaker antioxidant activity on this assay (Figure 5(C,D)).

Oxidation of HRG by peroxy radical

It is reported that albumin has antioxidant activity due to efficient self-oxidation. Because HRG also has the potential for producing antioxidant activity by self-oxidation, we investigated the oxidation of HRG by peroxy radicals. The degree of carbonylation on the Pro, Arg, Lys, and Thr residues in HRG was compared with HSA as an oxidation indicator. HRG was nearly twice as easy to be oxidized by peroxy radical as HSA (Figure 7(A)). We also determined the number of oxidized cysteine residues by detecting free-thiol. HSA has one free-thiol, and this free-thiol was oxidized by peroxy radical, whereas HRG showed no free-thiol (Figure 7(B)). Moreover, we tried to detect DT as oxidized tyrosine, and methionine sulfoxide as oxidized methionine in HSA or HRG treated with peroxy radical using western blotting method. We could not detect DT either in HSA or HRG treated with or without peroxy radicals (data not shown). On the contrary, methionine sulfoxide in

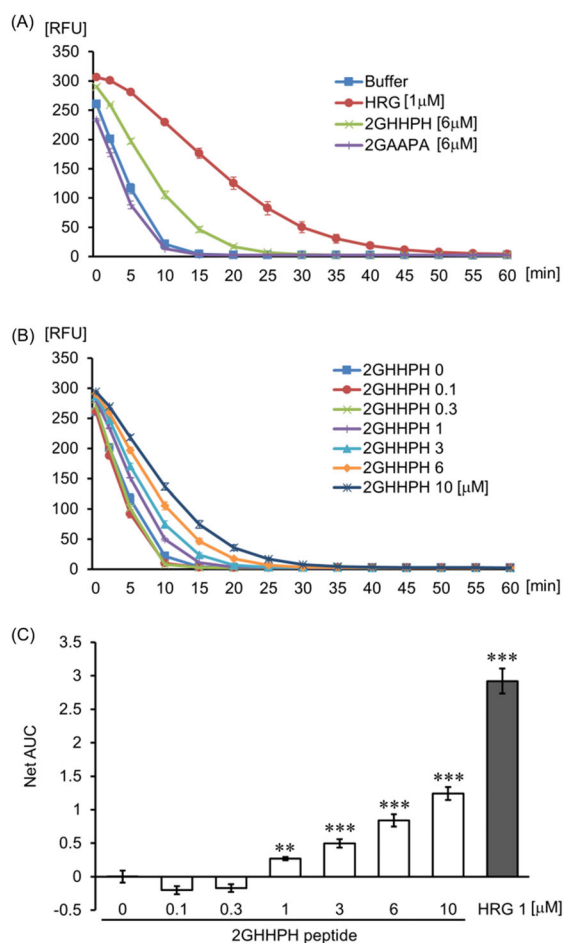


Figure 6. The effect of GHHPH peptide on peroxy radical. The quenching curve of the fluorescent probe in the group treated with PBS, HRG (1 μM), 2GHHPH (6 μM), and 2GAAPA (6 μM) (A) or in different concentrations of 2GHHPH (0–10 μM) (B). (C) The antioxidant capacity was calculated on the basis of the area under the fluorescent decay curve. The results shown are the means \pm SEM of three experiments. *** $p < 0.001$ vs. PBS (2GHHPH peptide 0 μM).

HSA was slightly increased by oxidation, although methionine sulfoxide was detected before oxidation by peroxy radicals (Figure 7(C)). Additionally, oxidized HRG, which did not show aggregation, exhibited a similar neutrophil rounding-inducing activity to non-oxidized HRG (Supporting Information Fig. 6). The data suggested that oxidization of HRG did not influence neutrophil rounding-inducing activity.

The influence of HRG on GPx reaction system

The GPx assay revealed that HRG has slight GPx-like activity (Figure 8(A)) and HRG enhanced the GPx activity significantly compared with PBS or HSA (Figure 8(B)). Additionally, to elucidate the binding affinity of HRG to GPxs (GPx1: cytosolic type, GPx3: plasma type and GPx4: phospholipid hydroperoxidase) which are associated with septic condition, we performed SPR assay. HRG binds to GPx1, GPx3, and GPx4 directly with high

affinity ($K_D = 6.946 \text{ E} - 8$, $2.662 \text{ E} - 8$, and $3.054 \text{ E} - 9$, respectively; Figure 8(C–E)).

Discussion

ROS include free radicals (superoxide [$\text{O}_2^{\cdot-}$], hydroxyl radicals [HO^{\cdot}], and peroxy radicals [ROO^{\cdot}]) and non-free radicals (hydrogen peroxide [H_2O_2] and lipid hydroperoxide [LOOH]). Hydroxyl radical plays a prominent role in the oxidation of protein, lipid, and nucleic acid *in vivo* because the oxidization ability of hydroxyl radicals is the highest among these ROS. Therefore, hydroxyl radical has been considered most important for the tissue injuries caused by ROS [35,36]. Moreover, lipid peroxy radicals (LOO^{\cdot}) produced by the oxidation of lipid bilayer of the cell membrane by hydroxyl radical triggers lipid peroxidation chain reaction and damages cell membranes [35]. In healthy conditions, the concentration of *in vivo* ROS is controlled by SOD and catalase, as well as the

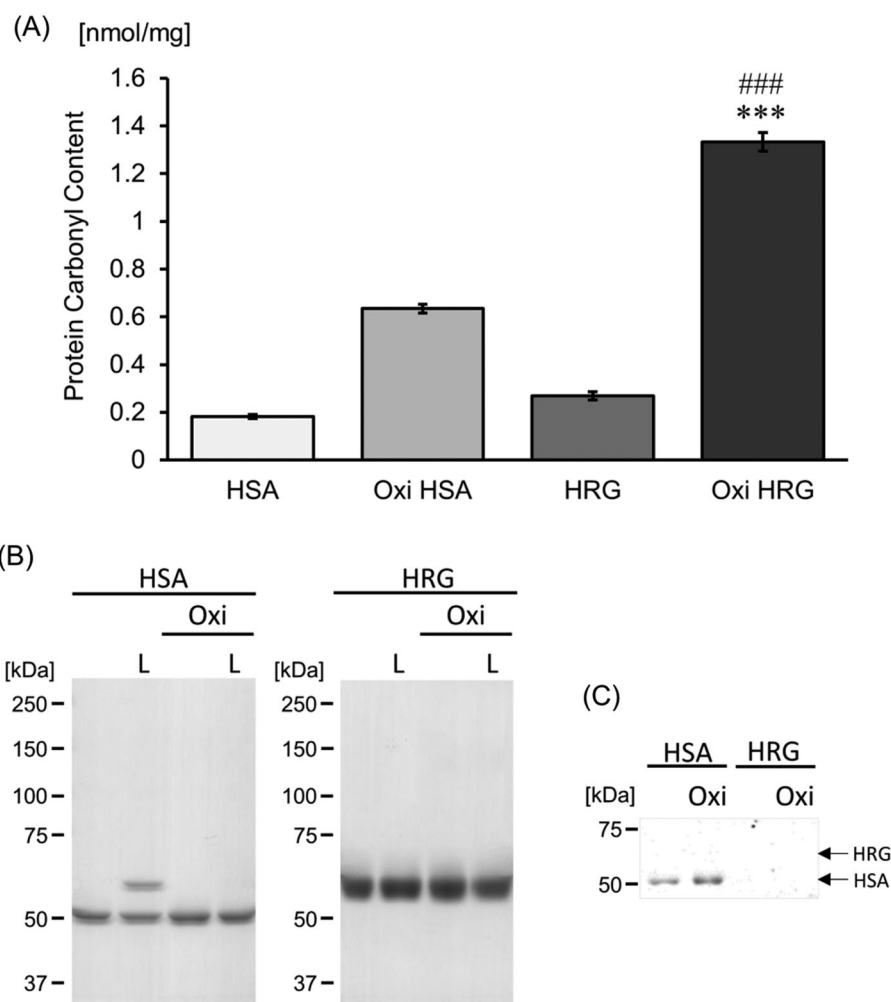


Figure 7. Detection of oxidized HRG by peroxy radicals. (A) The protein was oxidized by peroxy radicals produced by AAPH mixed with protein carbonyl fluorophore. The fluorescence was detected at Ex 485 nm/Em 530 nm. Protein concentration was determined using the Bradford assay, and the results were represented as nmol of protein carbonyl per mg of protein. The results shown are the means \pm SEM of three experiments. *** $p < 0.001$ vs. HRG. ### $p < 0.001$ vs. OxiHSA. (B) Modification of protein thiols was detected by SDS-PAGE. The protein thiols were labeled with Protein-SHifter (15 kDa), which has a maleimide group. (C) The protein methionine sulfoxide (MetO) as an oxidized methionine was detected with a rabbit anti-MetO polyclonal antibody. The same amount [(B): 5 ng, (C): 0.5 ng] of samples under non-reducing conditions were loaded on each lane.

glutathione-GPx system. For example, SOD catalyzes the dismutation of excess superoxide produced by NADPH oxidase or xanthine oxidase to hydrogen peroxide and oxygen, and the hydrogen peroxide is catalyzed and detoxified by catalase [35,36]. Additionally, GPx reduced hydrogen peroxide to water or LOOH to its corresponding alcohol. In contrast, there is increasing evidence that the uncontrolled generation of hydroxyl radical produced by divalent iron ion and hydrogen peroxide (Fenton's reaction) exacerbates different types of disease conditions, especially hemolysis, and cell damage related events such as sepsis [11,12,16–18,37].

In this study, we demonstrated that HRG was more effectively oxidized by radicals than albumin and

contributed to detoxifying not superoxide and hydrogen peroxide but peroxy radical that have high toxic activity. It is suggested that the self-oxidation tendency of HRG in inflammatory sites may protect the surrounding tissues from ROS damage. In addition to the antioxidant activity of HRG, we demonstrated that HRG enhanced the GPx activity, which is involved in detoxifying LOOH, although the detailed mechanism remains unclear. But, at least, HRG is suggested to modulate the GPx activity through its direct binding to GPxs. These results suggested that HRG contributes to antioxidant by a wide variety of its activities.

As aforementioned, hydroxyl radical is considered to be produced through Fenton's reaction in our body.

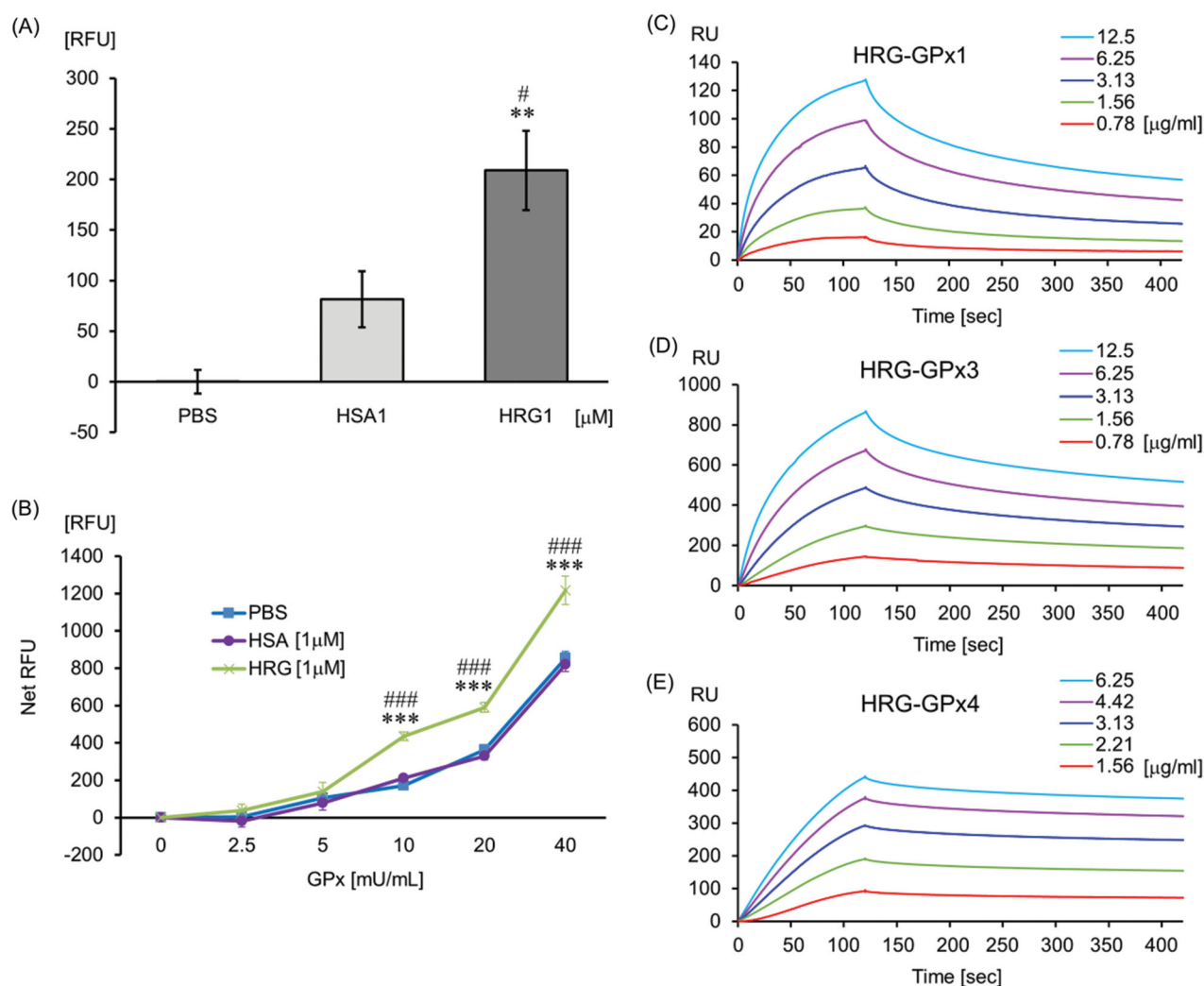


Figure 8. The influence of HRG on the glutathione peroxidase system. PBS, HSA ($1\mu\text{M}$), or HRG ($1\mu\text{M}$) (A) or GPx standard (0–40 mU/ml) with PBS, HSA ($1\mu\text{M}$), or HRG ($1\mu\text{M}$) (B) was mixed with kit solutions and incubated. The NADP probe reacted with NADP⁺-derived fluorescence was measured at Ex/Em = 420 nm/480 nm. The results shown are the means \pm SEM of three experiments. ** $p < 0.01$ and *** $p < 0.001$ vs. PBS. # $p < 0.05$ and ### $p < 0.001$ vs. HSA. SPR experiments were performed at 25 °C using Biacore T200 to determine the binding ability of HRG to - (C) GPx1, (D) GPx3, and (E) GPx4.

Fenton's reaction requires metal ions, for example, divalent iron ion, monovalent copper ion, and divalent cobalt ion, especially divalent iron ion is most important for this reaction [16–18]. Free-divalent iron ion is rigidly regulated by several proteins such as transferrin, lactoferrin, and ceruloplasmin in the bloodstream because its ion induces highly toxic hydroxyl radical production leading to tissue damage [38–41]. However, proteins binding to the divalent iron ion directly is not known in blood. Free divalent iron is generally oxidized by ceruloplasmin to trivalent iron, which binds to transferrin or lactoferrin and is metabolized [38,41]. However, direct binding to free divalent iron is thought to detoxify excess irons produced by tissue injury in

septic conditions, more effectively. Thus, understanding the underlying mechanism of regulation of high toxic-free divalent irons is essential.

For the first time, we discovered that HRG binds to 22 molecules of divalent iron ion directly and efficiently. Also, our results revealed that histidine residues inside the histidine-rich domain might play a critical role in the expression of divalent iron-chelating effect. The comparison of the chelating potencies between HRG and 2GHHPH peptides showed a six-fold difference, which could be attributed to the structure of HRG containing 12 repeats of GHHPH inside the histidine-rich domain.

It has been shown that the systemic inflammatory tissue damage and hemolysis in septic conditions

releases a huge amount of free divalent iron ions from the damaged cells [35,42–44], and with the progress in septic pathogenesis, the plasma HRG level was reduced due to rapid reduction in HRG gene expression, deposition of HRG on immunothrombi and degradation of HRG by thrombin [32]. Therefore, it is thought that free divalent iron ion is not able to be detoxified by HRG effectively in the reduction phase of plasma HRG levels in sepsis. Indeed, the reduction of plasma HRG level has been reported to correlate with an adverse progress of septic patients [33]. From these reports and our data, it was speculated that HRG may contribute to preventing cell damage at least in part *via* its divalent iron-chelating effect in sepsis.

In conclusion, the present study suggested that in septic conditions, HRG can inhibit the production of hydroxyl radical, enhance GPx activity, and remove peroxyl radical and free divalent metal ions efficiently, indicating the potential of HRG to exert the antiseptic effects *in vivo* in addition to the cellular regulation of neutrophils, erythrocytes, and vascular endothelial cells [45].

Acknowledgments

Human fresh frozen plasma was kindly provided by the Japanese Red Cross Society. We would like to thank Editage (www.editage.com) for English language editing.

Author contributions

H.W., S.M., and M.N. planned the study; H.W., Y.T., Y.Y., and D.W. performed the antioxidant capacity activity assays; H.W., K.T., and S.G. performed the experiments using ITC and Biacore; H.W. performed the experiments of detecting oxidized protein; H.W., S.M., and M.N. wrote the manuscript.

Disclosure statement

No potential conflict of interest was reported by the author(s).

Funding

This work was supported by AMED [grant no. 18im0210109h0002], JSPS KAKENHI [grant no. 15H04686], and Secom Science and Technology Foundation to M.N. and JSPS KAKENHI [grant no. 17K15580] and Teraoka Memorial Scholarship Society Foundation to H.W.

References

- [1] Genga KR, Russell JA. Update of sepsis in the intensive care unit. *J Innate Immun.* 2017;9(5):441–455.
- [2] Perner A, Gordon AC, De Backer D, et al. Sepsis: frontiers in diagnosis, resuscitation and antibiotic therapy. *Intensive Care Med.* 2016;42(12):1958–1969.
- [3] Fink MP, Warren HS. Strategies to improve drug development for sepsis. *Nat Rev Drug Discov.* 2014;13(10):741–758.
- [4] Opal SM, Laterre PF, Francois B, et al. Effect of eritoran, an antagonist of MD2-TLR4, on mortality in patients with severe sepsis: the ACCESS randomized trial. *JAMA.* 2013;309(11):1154–1162.
- [5] Ranieri VM, Thompson BT, Barie PS, et al. Drotrecogin alfa (activated) in adults with septic shock. *N Engl J Med.* 2012;366(22):2055–2064.
- [6] Rice TW, Wheeler AP, Bernard GR, et al. A randomized, double-blind, placebo-controlled trial of TAK-242 for the treatment of severe sepsis. *Crit Care Med.* 2010;38(8):1685–1694.
- [7] Gaieski DF, Edwards JM, Kallan MJ, et al. Benchmarking the incidence and mortality of severe sepsis in the United States. *Crit Care Med.* 2013;41(5):1167–1174.
- [8] Kaukonen KM, Bailey M, Suzuki S, et al. Mortality related to severe sepsis and septic shock among critically ill patients in Australia and New Zealand, 2000–2012. *JAMA.* 2014;311(13):1308–1316.
- [9] Dellinger RP, Levy MM, Rhodes A, et al. Surviving sepsis campaign: international guidelines for management of severe sepsis and septic shock: 2012. *Crit Care Med.* 2013;41(2):580–637.
- [10] Semeraro N, Ammollo CT, Semeraro F, et al. Sepsis, thrombosis and organ dysfunction. *Thromb Res.* 2012;129(3):290–295.
- [11] Delabranche X, Helms J, Meziani F. Immunohaemostasis: a new view on haemostasis during sepsis. *Ann Intensive Care.* 2017;7(1):117.
- [12] Frantzeskaki F, Armaganidis A, Orfanos SE. Immunothrombosis in acute respiratory distress syndrome: cross talks between inflammation and coagulation. *Respiration.* 2017;93(3):212–225.
- [13] Singer M, Deutschman CS, Seymour CW, et al. The Third International Consensus Definitions for Sepsis and Septic Shock (Sepsis-3). *JAMA.* 2016;315(8):801–810.
- [14] Yipp BG, Kubes P. NETosis: how vital is it? *Blood.* 2013;122(16):2784–2794.
- [15] Brinkmann V, Reichard U, Goosmann C, et al. Neutrophil extracellular traps kill bacteria. *Science.* 2004;303(5663):1532–1535.
- [16] Andrades ME, Ritter C, Dal-Pizzol F. The role of free radicals in sepsis development. *Front Biosci (Elite Ed).* 2009;1:277–287.
- [17] Fialkow L, Wang Y, Downey GP. Reactive oxygen and nitrogen species as signaling molecules regulating neutrophil function. *Free Radic Biol Med.* 2007;42(2):153–164.
- [18] Huet O, Dupic L, Harrois A, et al. Oxidative stress and endothelial dysfunction during sepsis. *Front Biosci (Landmark Ed).* 2011;16:1986–1995.
- [19] Koide T, Foster D, Yoshitake S, et al. Amino acid sequence of human histidine-rich glycoprotein derived from the nucleotide sequence of its cDNA. *Biochemistry.* 1986;25(8):2220–2225.

- [20] Poon IK, Patel KK, Davis DS, et al. Histidine-rich glycoprotein: the Swiss Army knife of mammalian plasma. *Blood*. 2011;117(7):2093–2101.
- [21] Borza DB, Tatum FM, Morgan WT. Domain structure and conformation of histidine-proline-rich glycoprotein. *Biochemistry*. 1996;35(6):1925–1934.
- [22] Leung LL. Interaction of histidine-rich glycoprotein with fibrinogen and fibrin. *J Clin Invest*. 1986;77(4):1305–1311.
- [23] Lijnen HR, Hoylaerts M, Collen D. Heparin binding properties of human histidine-rich glycoprotein. Mechanism and role in the neutralization of heparin in plasma. *J Biol Chem*. 1983;258(6):3803–3808.
- [24] Peterson CB, Morgan WT, Blackburn MN. Histidine-rich glycoprotein modulation of the anticoagulant activity of heparin. Evidence for a mechanism involving competition with both antithrombin and thrombin for heparin binding. *J Biol Chem*. 1987;262(16):7567–7574.
- [25] Silverstein RL, Leung LL, Harpel PC, et al. Platelet thrombospondin forms a trimolecular complex with plasminogen and histidine-rich glycoprotein. *J Clin Invest*. 1985;75(6):2065–2073.
- [26] Bosshart H, Heinzelmann M. Endotoxin-neutralizing effects of histidine-rich peptides. *FEBS Lett*. 2003;553(1–2):135–140.
- [27] Poon IK, Hulett MD, Parish CR. Histidine-rich glycoprotein is a novel plasma pattern recognition molecule that recruits IgG to facilitate necrotic cell clearance via FcγRI on phagocytes. *Blood*. 2010;115(12):2473–2482.
- [28] Tugues S, Roche F, Noguier O, et al. Histidine-rich glycoprotein uptake and turnover is mediated by mononuclear phagocytes. *PLoS One*. 2014;9(9):e107483.
- [29] Zhong H, Wake H, Liu K, et al. Effects of histidine-rich glycoprotein on erythrocyte aggregation and hemolysis: implications for a role under septic conditions. *J Pharmacol Sci*. 2018;136(3):97–106.
- [30] Morgan WT. The histidine-rich glycoprotein of serum has a domain rich in histidine, proline, and glycine that binds heme and metals. *Biochemistry*. 1985;24(6):1496–1501.
- [31] Priebatsch KM, Poon IK, Patel KK, et al. Divalent metal binding by histidine-rich glycoprotein differentially regulates higher order oligomerisation and proteolytic processing. *FEBS Lett*. 2017;591(1):164–176.
- [32] Wake H, Mori S, Liu K, et al. Histidine-rich glycoprotein prevents septic lethality through regulation of immunothrombosis and inflammation. *EBioMedicine*. 2016;9:180–194.
- [33] Kuroda K, Wake H, Mori S, et al. Decrease in histidine-rich glycoprotein as a novel biomarker to predict sepsis among systemic inflammatory response syndrome. *Crit Care Med*. 2018;46(4):570–576.
- [34] Mori S, Takahashi HK, Yamaoka K, et al. High affinity binding of serum histidine-rich glycoprotein to nickel-nitrilotriacetic acid: the application to microquantification. *Life Sci*. 2003;73(1):93–102.
- [35] Valko M, Jomova K, Rhodes CJ, et al. Redox- and non-redox-metal-induced formation of free radicals and their role in human disease. *Arch Toxicol*. 2016;90(1):1–37.
- [36] Zuo L, Zhou T, Pannell BK, et al. Biological and physiological role of reactive oxygen species—the good, the bad, and the ugly. *Acta Physiol (Oxf)*. 2015;214(3):329–348.
- [37] Mittal M, Siddiqui MR, Tran K, et al. Reactive oxygen species in inflammation and tissue injury. *Antioxid Redox Signal*. 2014;20(7):1126–1167.
- [38] Ganz T. Systemic iron homeostasis. *Physiol Rev*. 2013;93(4):1721–1741.
- [39] Hentze MW, Muckenthaler MU, Galy B, et al. Two to tango: regulation of mammalian iron metabolism. *Cell*. 2010;142(1):24–38.
- [40] Martins AC, Almeida JI, Lima IS, et al. Iron metabolism and the inflammatory response. *IUBMB Life*. 2017;69(6):442–450.
- [41] Sill C, Biehl R, Hoffmann B, et al. Structure and domain dynamics of human lactoferrin in solution and the influence of Fe(III)-ion ligand binding. *BMC Biophys*. 2016;9:7.
- [42] Takami T, Sakaida I. Iron regulation by hepatocytes and free radicals. *J Clin Biochem Nutr*. 2011;48(2):103–106.
- [43] Lv H, Shang P. The significance, trafficking and determination of labile iron in cytosol, mitochondria and lysosomes. *Metallomics*. 2018;10(7):899–916.
- [44] Nemeth E, Tuttle MS, Powelson J, et al. Hepcidin regulates cellular iron efflux by binding to ferroportin and inducing its internalization. *Science*. 2004;306(5704):2090–2093.
- [45] Wake H. Histidine-rich glycoprotein modulates the blood-vascular system in septic condition. *Acta Med Okayama*. 2019;73(5):379–382.